

Supporting information for: **The importance of correcting for variable probe - sample interactions in AFM-IR spectroscopy: AFM-IR of dried bacteria on a polyurethane film**

Daniel E. Barlow,<sup>1\*</sup> Justin C. Biffinger,<sup>1</sup> Allison L. Cockrell-Zugell,<sup>2</sup> Michael Lo,<sup>3</sup> Kevin Kjoller,<sup>3</sup> Debra Cook,<sup>3</sup> Woo Kyung Lee,<sup>1</sup> Pehr E. Pehrsson,<sup>1</sup> Wendy J. Crookes-Goodson,<sup>4</sup> Chia-Suei Hung,<sup>4</sup> Lloyd J. Nadeau,<sup>4</sup> John N. Russell, Jr.<sup>1</sup>

<sup>1</sup> Chemistry Division, Naval Research Lab, Washington, DC 20375

<sup>2</sup> National Research Council Post-doctoral Research Associate

<sup>3</sup> Anasys Instruments, Inc., Santa Barbara, CA

<sup>4</sup> Soft Matter Materials Branch, Materials & Manufacturing Directorate, Air Force Research Laboratory, Wright-Patterson AFB, OH 45433

\*Corresponding author

Email: daniel.barlow@nrl.navy.mil

### Force – distance measurements

Force – distance measurements were obtained from the same sample used for AFM-IR analysis of *Pseudomonas protegens* Pf-5 bacteria (Pf) on the polyether – polyurethane (PU) film. They were acquired using a Bruker Dimension 3000 AFM, Nanoscope V controller, and a Bruker SNL-10 probe (silicon tip on nitride lever). Thermal tune analysis using the Bruker Nanoscope 7.3 software indicated a cantilever spring constant of 0.56 N/m. Figure SI 1 compares the AFM force – distance curves acquired from Pf and PU, showing that PU is more compliant and plastically deformed relative to Pf for the applied force. This also demonstrates higher energy dissipation in the PU material.

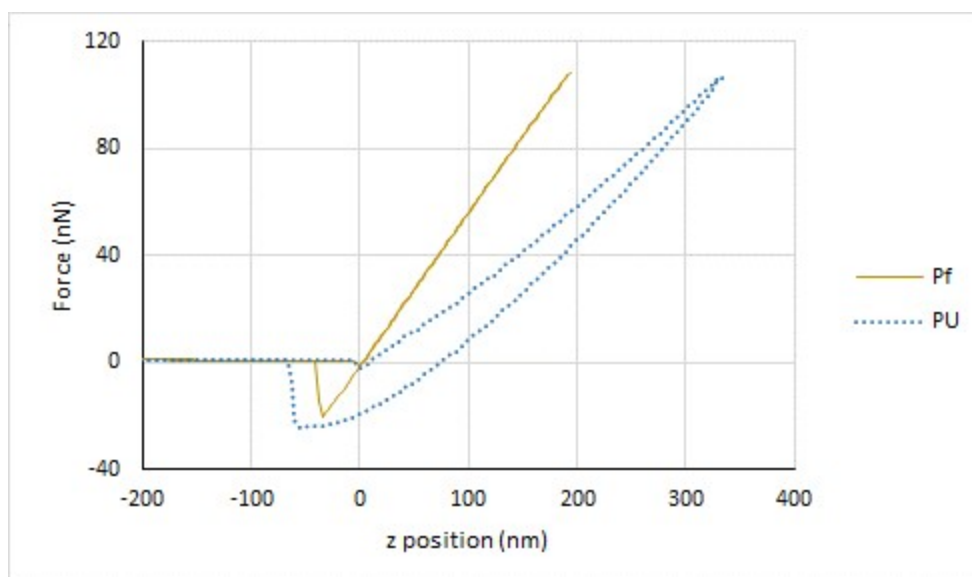


**Figure S11.** Comparison of AFM force –distance curves acquired on *P. protegens* Pf-5 (Pf) and polyurethane (PU).

### AFM-IR measurements at 2282 kHz contact resonance

Figure S12(a,b) shows comparisons of IR laser – tip alignment maps with the cantilever ring-down filtered at 2282 kHz (200 kHz filter width) and 89 kHz (20 kHz filter width), respectively. These were acquired by positioning the tip on a bacteria – PU bilayer region and scanning the IR laser position relative to the tip and plotting the ring-down peak intensities. The IR laser was tuned to  $1732\text{ cm}^{-1}$  and except for the differences in bandpass filter and deflection gains, all the settings were identical. This procedure optimizes alignment of the tip and laser, with the alignment set at the location with the maximum peak intensity. Comparison of the two maps shows that detection of thermal expansion is much more localized at the tip at 89 kHz, where at 2282 kHz a higher relative amount of thermal expansion can be detected underneath the cantilever as well by a through – air signal. The laser spot size is larger than the tip, so even with the laser and tip aligned it could be possible to detect thermal expansion beyond the tip location. As an additional note, IR laser – tip alignment maps acquired with the probe in contact with PU versus Pf-PU was also found to affect the relative signal measured at the tip versus the through air signal. When in contact with PU (not shown), the signal at the tip decreased relative to the signal under the cantilever. This occurred at both the 2282 kHz and 89 kHz frequencies, and is likely another effect of different mechanical interactions between the tip and sample.

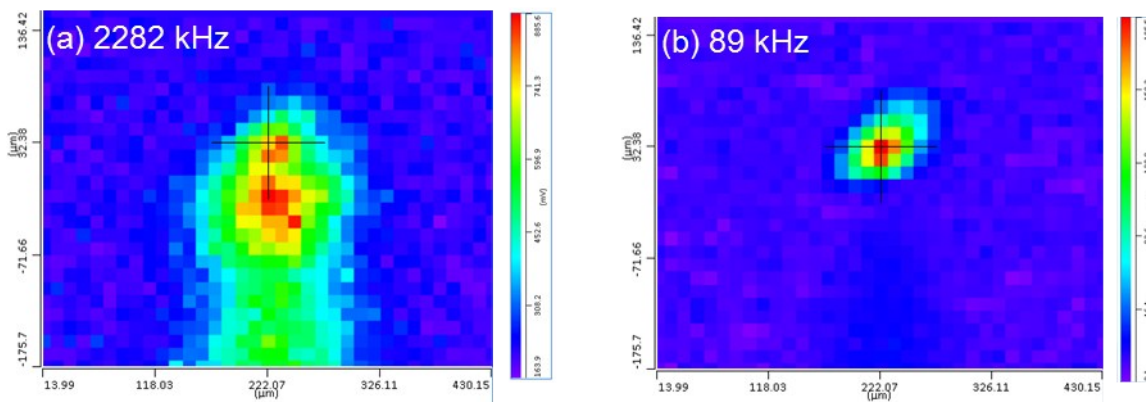


**Figure S12.** Comparison of IR laser – tip alignment maps with the cantilever ring-down filtered at (a) 2282 kHz and (b) 89 kHz. Except for differences in bandpass filter frequencies and deflection gain, the maps were acquired under identical conditions with the tip positioned on bacteria over PU and the IR laser tuned to  $1732\text{ cm}^{-1}$ . The tip is located approximately at the crosshairs, and the cantilever extends from the bottom of the images.

Figure S13 shows the resulting AFM-IR spectra acquired with band-pass filtering at 2282 kHz. Spectra were acquired with the tip either on Pf-PU or PU and are shown with the peak intensities measured from either the FFT amplitudes at 2282 kHz (S13(a)) or the maximum peak – peak intensities in the filtered ring-down

(SI3(b)). Figure SI3(a) shows that the spectra are very similar with the tip positioned on either Pf or PU, mostly reflecting features from PU with only a small increased absorbance at the Pf amide I frequency. The similar intensities at  $1732\text{ cm}^{-1}$  are as expected based on the frequency spectrum in Figure 4(b). Unfortunately, the expected relative peak intensity differences for PU and Pf-PU are not observed. This is attributed to loss of spatial resolution, in agreement with the results in Figure SI2, with the spectra reflecting the sparsely bacteria covered PU coating. Figure SI3(b) shows the spectra from the same measurement, but based on the maximum peak – peak intensities as with the spectra in Figure 2. While this shows slightly improved sensitivity to the amide I mode with the tip on Pf-PU, it is still significantly reduced in comparison to Figure 2(b). Furthermore, the anomalous  $1732\text{ cm}^{-1}$  intensity difference recurs. Thus, working at this high frequency contact resonance unfortunately does not help solve the issue of obtaining high spatial resolution AFM-IR with decreased sensitivity to dissipative variations.

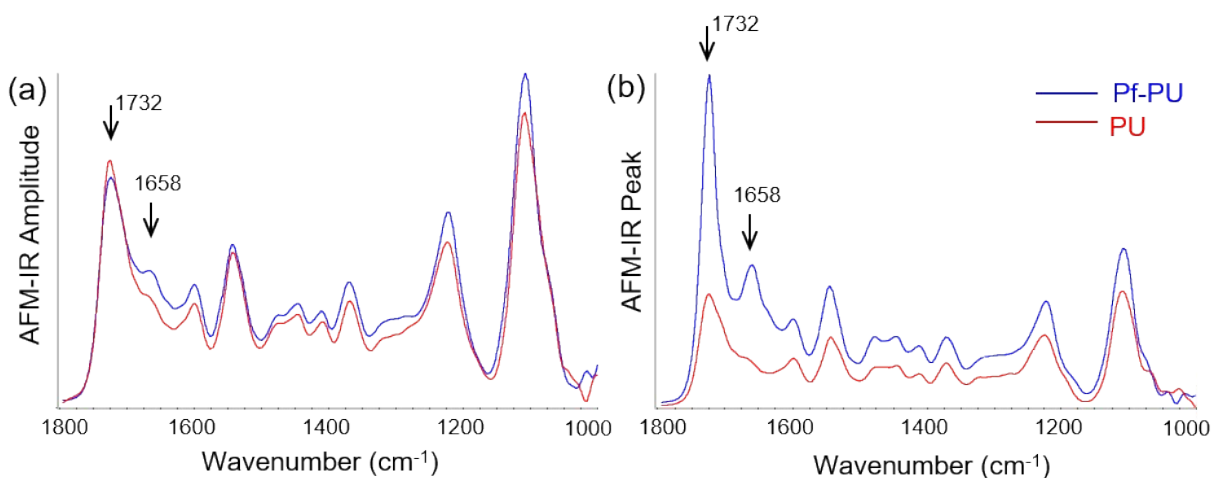


Figure SI3. AFM-IR spectra acquired with band-pass filtering at 2282 kHz. Peak intensities were measured from (a) the FFT amplitudes at 2282 kHz and (b) the maximum peak – peak intensities in the filtered ring-down.